Electron-Nuclear Double-Resonance of Interstitial Positively Charged Iron in Silicon

Vankooten, J.J.; Sieverts, E.G.; Ammerlaan, C.A.J.

DOI
10.1103/PhysRevB.37.8949

Publication date
1988

Published in
Physical Review. B, Condensed Matter

Electron-nuclear double resonance of interstitial positively charged iron in silicon

J. J. van Kooten, E. G. Sieverts, and C. A. J. Ammerlaan
Natuurkundig Laboratorium der Universiteit van Amsterdam, Valckenierstraat 65, NL-1018 XE Amsterdam, The Netherlands
(Received 2 November 1987)

The positively charged state of interstitial iron in silicon was studied by means of electron-nuclear double resonance. We have found hyperfine interactions of the impurity electrons with eight shells of silicon neighbors containing 98 atoms. Because the ground state of interstitial Fe^+ is orbitally degenerate, it has quite different features than interstitial Fe^0, Ti^+, and Cr^+ in silicon. The analysis of the hyperfine interactions is much more complicated because the ground state cannot be written as a single Slater determinant. For the most important high-symmetry ligand hyperfine interactions a complete analysis with proper orbitally degenerate wave functions has been carried out. For more remote lower-symmetry neighbor sites the experimental data indicate prominence of σ-type ligand orbitals. It is derived that the total spin density transferred to the surrounding silicon atoms is at least 26%. Recent theoretical calculations are found to be in good agreement with this experimental result.

I. INTRODUCTION

Because of its high diffusion coefficient, iron is often unintentionally present in silicon. The iron solubility of 10^{16} cm^{-3} (Ref. 1) is sufficiently high to study iron with various measuring techniques. Not surprisingly, iron is one of the most studied transition metals in silicon. Iron introduces a donor level in the gap ($Fe^0 \rightarrow Fe^+$) at 0.385 eV above the valence band. Like most transition metals, iron is present at the interstitial T site after rapid quenching from the diffusion temperature. In electron paramagnetic resonance (EPR) both the neutral and singly positive charge state of interstitial iron are identified. In heavily doped p-type material no resonance of Fe_i^+ is observed, although no EPR resonance which can be associated with $Si{:}Fe_i^{2+}$ is perceived either. The EPR characteristics are conveniently described by the Ludwig- and Woodbury model:[2,3] The s electrons are transferred to the d shell which is split by the cubic field in an upper e and a lower t_2 shell. The levels are filled according to Hund's rule, i.e., the configuration with highest spin constitutes the ground state. In the case of interstitial Fe^+ with electronic configuration $(3d)^7$, the t_2 shell is only partly filled and the ground state is $^4T_1$. Therefore orbital momentum is still present, and this implies that Fe_i^+ (and Mn_i^0) has different features than other well-known transition metals in silicon. This remaining orbital momentum is described by an effective spin $L'=1$. The orbital momentum and the spin moment $S=\frac{3}{2}$ are coupled to give $J=\frac{1}{2},\frac{3}{2},\frac{5}{2}$ states of which the Kramers doublet $J=\frac{1}{2}$ constitutes the ground state. The remaining orbital momentum also contributes to the g factor with $g_{L'}=-\frac{3}{2}$. If all orbital momentum would contribute one would expect $g=\frac{5}{3}g_S-\frac{2}{3}g_{L'}$ which equals $\frac{13}{3}$; for complete absence of orbital contributions $g=\frac{10}{3}$. Experimentally one finds $g=3.524$,[2] which is only slightly higher than the value for complete quenching. An explanation for this deviation was first given by Ham.[4,5] Since the ground state of Fe_i^+ ($^4T_1$) is orbitally degenerate, a Jahn-Teller distortion is expected. The EPR spectrum of Fe_i^+ is isotropic, indicating cubic symmetry for the center, excluding any sizable static distortion. According to the theoretical interpretation, a dynamical Jahn-Teller effect partially quenches the orbital contribution to the g factor and accounts for the experimental value $g=3.524$.

However, recent theoretical calculations[6-9] show that covalency cannot be neglected even in the case of a deep defect like Fe. Covalency also reduces the contribution of orbital magnetism and can account for the reduction in g value as well. From EPR measurements of iron-acceptor pairs one can conclude that covalency is more important than the dynamical Jahn-Teller effect.[10,11]

As indicated by Katayama-Yoshida and Zunger[6-8] there seems to be a duality with respect to localization for Si:Fe. A localized picture is supported by the ground-state total momentum $J=\frac{1}{2}$, by the absence of a static Jahn-Teller distortion despite the $^4T_1$ ground state for Fe_i^+, and by the fast diffusivity. Arguments in favor of a delocalized model are the strong crystal field, the reduction in central-ion hyperfine interaction and the reduction of the s-d Coulomb repulsion allowing the transfer of an s electron to the d shell.

Katayama-Yoshida and Zunger did calculate the electronic structure of interstitial iron (both neutral and positively charged) by means of a self-consistent, all-electron, spin-polarized Green's-function method. Experimentally the appropriate technique to measure the localization of the electron state of a defect is electron-nuclear double resonance (ENDOR). ENDOR results for Fe_i^0 are published in Ref. 12, and additional experimental data and a different interpretation of these data are found in Ref. 13. In this paper we present our ENDOR results of Fe_i^+.

II. EXPERIMENTAL PROCEDURE

Starting material for the samples was float-zone-grown dislocation-free 0.9 Ω cm p-type silicon supplied by Wacker Chemitronic. Material of this resistivity yielded the highest concentration of Fe_i^+. Iron was introduced

in the silicon by scraping with a piece of etched iron over the sample surface[14] followed by diffusion in a closed quartz ampoule under argon atmosphere at the temperature of 1300 °C for about 3 h. The samples were slowly cooled, ground, and etched. After subsequent heating at 1300 °C for a short period in an open ampoule the samples were quenched in water. Typical dimensions of the samples were $2\times2\times15$ mm^3. Until the measurements the samples were stored in liquid nitrogen. Even a short period at room temperature is enough to reduce the interstitial iron concentration due to the formation of iron clusters and iron-acceptor pairs. Many samples were prepared because the EPR intensity and line shape were very sample dependent. The measurements were performed in a superheterodyne K-band spectrometer. The incident microwave power was 1 μW and the spectrometer was tuned to dispersion. The magnetic field could be rotated in a {011} plane and was modulated at 83 Hz. The cylindrical TE_{011} cavity was made of silver-coated Epibond. In the wall a spiral groove was cut to make it operate as an rf coil. The rf power was on-off modulated at a frequency of 3 Hz, and the signal was detected by two lock-in amplifiers to allow double phase-sensitive detection. The ENDOR measurements were performed at a temperature of 2 K.

III. RESULTS

The electron-paramagnetic-resonance line of interstitial Fe^+ in silicon is a strain-broadened transition

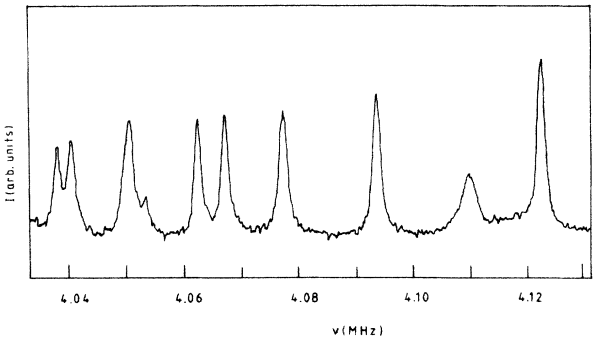

FIG. 1. Recorder trace of an electron nuclear double resonance spectrum for Si:Fe_i^+. The magnetic field is parallel to [100].

$\Delta m_J=\pm1$ for a $J=\frac{1}{2}$ system with isotropic g value $g=3.524$. The full width at half maximum of the EPR transition is typically of the order of 0.8 mT. This width is strongly angular dependent and is smallest for fields in the ⟨100⟩ directions.[15] For comparison, the EPR line of Si:Fe_i^0 is always narrowest in the ⟨111⟩ directions. Contrary to Si:Fe_i^0,[16] no hyperfine structure due to interaction with ^{29}Si could be resolved in EPR for Fe_i^+.

An example of an ENDOR spectrum is given in Fig. 1. The linewidth of the ENDOR resonances was of the order of 2 kHz. The iron ions are situated at the T-interstitial positions in the silicon lattice, which have site

TABLE I. Hyperfine tensors ($\overleftrightarrow{A}$), principal values A_i, and eigenvectors ($\mathbf{n}_i$) of ^{29}Si neighbors of Si:Fe_i^+. Experimental uncertainty is 0.4 kHz.

Tensor	$\overleftrightarrow{A}$ (kHz)			i	A_i (kHz)	$\mathbf{n}_i$
T1	764.0	−226.4	−226.4	1	990.4	(0.408, 0.408, −0.817)
	−226.4	764.0	−226.4	2	990.4	(0.707, −0.707, 0.000)
	−226.4	−226.4	764.0	3	311.3	(0.577, 0.577, 0.577)
T2	87.6	1230.8	1230.8	1	2549.1	(0.577, 0.577, 0.577)
	1230.8	87.6	1230.8	2	−1143.2	(0.408, 0.408, −0.817)
	1230.8	1230.8	87.6	3	−1143.2	(0.707, −0.707, 0.000)
R1	6790.7	460.0	0.0	1	9006.5	(0.000, 0.000, 1.000)
	460.0	6790.7	0.0	2	7250.7	(0.707, 0.707, 0.000)
	0.0	0.0	9006.5	3	6330.6	(0.707, −0.707, 0.000)
M1	3639.3	71.4	538.0	1	4963.9	(0.367, 0.367, 0.855)
	71.4	3639.3	538.0	2	3567.9	(0.707, −0.707, 0.000)
	538.0	538.0	4502.1	3	3248.9	(0.604, 0.604, −0.519)
M2	357.4	361.8	83.8	1	748.0	(0.687, 0.687, 0.236)
	361.8	357.4	83.8	2	231.0	(0.167, 0.167, −0.972)
	83.8	83.8	259.8	3	−4.4	(0.707, −0.707, 0.000)
M3	592.2	96.2	142.2	1	830.1	(0.578, 0.578, 0.576)
	96.2	592.2	142.2	2	496.0	(0.707, −0.707, 0.000)
	142.2	142.2	544.7	3	403.0	(0.407, 0.407, −0.818)
G1	227.6	77.2	81.4	1	492.1	(0.385, 0.497, 0.778)
	77.2	283.1	95.5	2	237.1	(0.353, 0.699, −0.622)
	81.4	95.5	390.7	3	172.2	(0.853, −0.514, −0.094)
G2	194.1	3.6	77.2	1	889.8	(0.095, 0.549, 0.830)
	3.6	353.3	354.5	2	205.5	(0.909, −0.387, 0.152)
	77.2	354.5	646.5	3	98.6	(0.405, 0.740, −0.536)

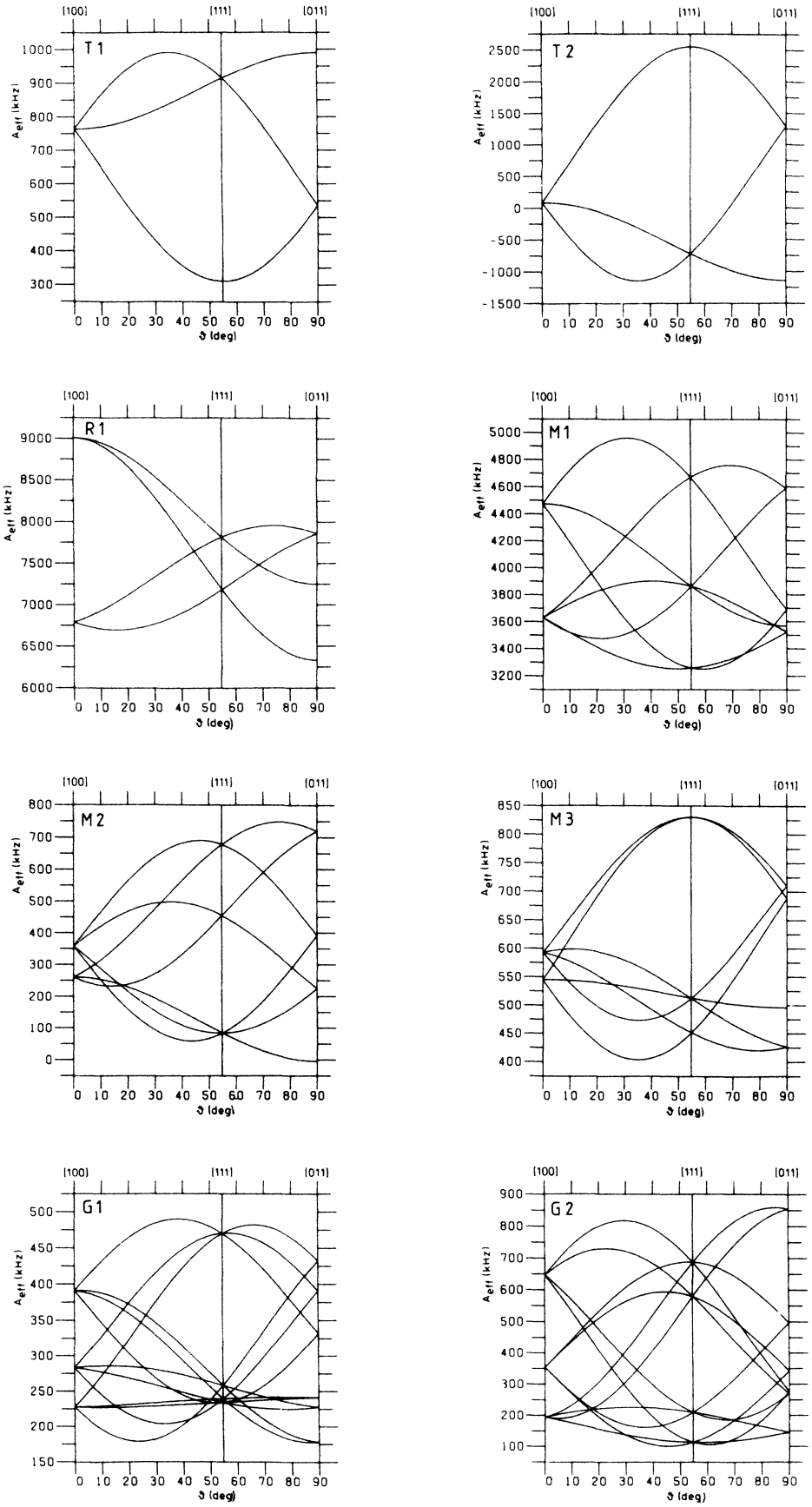

FIG. 2. Angular dependencies of the effective hyperfine interaction A_{eff} for rotation of the magnetic field in the $(0\bar{1}1)$ plane, for all eight observed ligand hyperfine interactions.

symmetry $\bar{4}3m$. The silicon neighbor sets can be divided into four symmetry classes: General class containing 24 atoms per shell (labeled G), mirror-plane ($\{011\}$) class containing 12 atoms per shell (labeled M), rhombic I ($\langle 100\rangle$) class with 6 atoms per shell (labeled R), and trigonal ($\langle 111\rangle$) class with 4 atoms per shell (labeled T). The separate atoms within a shell are equivalent by the $\bar{4}3m$ symmetry. Each symmetry class gives a different number of ENDOR lines with a characteristic angular dependence. We resolved eight hyperfine interaction tensors: one rhombic, two trigonal, three mirror-plane and two general class tensors. In Fig. 2 the angle-dependent patterns of the eight hyperfine interaction tensors are depicted. All spectra could be analyzed with the following spin Hamiltonian:

$$\mathcal{H}=g_e\mu_B\mathbf{B}\cdot\mathbf{J}+\sum_i(\mathbf{J}\cdot\overleftrightarrow{\mathbf{A}}_i\cdot\mathbf{I}_i-g_N\mu_N\mathbf{B}\cdot\mathbf{I}_i)\ . \tag{1}$$

The first term describes the electronic Zeeman interaction, the last the nuclear Zeeman interaction, and the middle term the hyperfine interaction. The summation is over the lattice sites where a ^{29}Si nucleus is situated. The abundance of the magnetic isotope ^{29}Si is 4.7%. The ENDOR spectra could be described with an effective spin $J=\frac{1}{2}$ and the nuclear spin $I=\frac{1}{2}$ of ^{29}Si. The parameters to be determined are the components of $\overleftrightarrow{\mathbf{A}}$. The ENDOR transitions ($\Delta m_I=\pm1$) are given in first order as

$$h\nu=|\,g_N\mu_N B-A_{\text{eff}}m_J\,|\ , \tag{2}$$

with $A_{\text{eff}}=\mathbf{B}\cdot\overleftrightarrow{\mathbf{A}}\cdot\mathbf{B}/B^2$ and $m_J=\pm\frac{1}{2}$. The ENDOR spectrum is thus symmetric around the nuclear Zeeman frequency $g_N\mu_B B/h$. The measured ENDOR spectra were fitted to the components of $\overleftrightarrow{\mathbf{A}}$ by means of diagonalization of the matrix representation of Eq. (1). The deviation between calculated and measured frequencies was generally within the ENDOR linewidth. The results are shown in Table I. Tensor elements are given with respect to Cartesian coordinates. Furthermore, the principal values and eigenvectors are given. It is noted that the overall sign of the elements could not be determined experimentally. An identification of a hyperfine tensor to a specific shell of atoms is not possible on the basis of the experimental data only.

IV. ANALYSIS

Our purpose is to derive from the measured hyperfine tensors an estimate for the spin density which is transferred from the central metal ion to the silicon ligands. Most simply, the data can be analyzed by the traditional one-electron LCAO approach of Watkins and Corbett.[17] In this analysis the tensor is written as $\overleftrightarrow{\mathbf{A}}=a\overleftrightarrow{\mathbf{1}}+\overleftrightarrow{\mathbf{B}}$, with $a=\frac{1}{3}\mathrm{Tr}(\overleftrightarrow{\mathbf{A}})$. An electron in a ligand $3s$ orbital causes an isotropic hyperfine interaction with $a=4594$ MHz, and an electron in a $3p$ orbital gives a traceless axially symmetric tensor $\overleftrightarrow{\mathbf{B}}$ with principal values $(+2b,-b,-b)$ and $b=114.2$ MHz.[18] This analysis yields for the eight hyperfine tensors a total transferred spin density of 28%. Data relevant to this analysis are summarized in Table II. The constants a, b, and c in Table II are related to the principal values of $\overleftrightarrow{\mathbf{A}}$ by equating these values to $a+2b$, $a-b+c$, and $a-b-c$. In the case of a transition-metal ion in silicon, this model can only be used as a first approximation, because it does not take into account (a) the proper more-electron ground state of the defect, (b) the correct symmetry of the molecular orbital, and (c) dipole-dipole interaction with spin densities at other atom sites, especially at the central ion.

A hyperfine tensor with different signs for the isotropic and anisotropic parts, as shown in Table II for tensor T1, can, for instance, never be explained within this model. Therefore, a more detailed model is required for description of the influence of covalency on the magnetic properties of Fe_i^+ in silicon. For transition metals with a first-order quenching of the orbital momentum, the basic theory is described by Owen and Thornley.[19] For silicon this model was applied to interstitial Ti^+ ($3d^3$), Fe^0 ($3d^8$), and Cr^+ ($3d^5$).[13,20,21] Because it has an orbitally degenerate and thus no single-determinant ground state, the case of interstitial Fe^+ is more complicated and necessitates the calculation of the hyperfine interactions from first principles.[19] This method was developed by Thornley *et al.*[22] to describe the properties of Co^{2+} ($3d^7$) in octahedral salts, for instance $KMgF_3$:Co. The methods of analysis reported in Refs. 19 and 22 are also discussed in Ref. 23. Our analysis of interstitial Fe^+ in silicon ($\bar{4}3m$ symmetry) will closely follow this approach.[22,23] In these references also the notation is defined.

TABLE II. One-electron LCAO analysis of the Si:Fe^+ hyperfine interactions. Units of a, b, and c are kHz. α^2 is the fraction s character, β^2 the fraction p character, η^2 the localization per atom, and n the number of atoms in a shell.

Tensor	a	b	c	a/b	b/c	α^2	β^2	η^2 (%)	$n\eta^2$ (%)
T1	764.0	−226.4	0.0	−3.37		0.077	0.923	0.22	0.86
T2	87.6	1230.8	0.0	0.07		0.002	0.998	1.08	4.32
R1	7529.3	738.6	460.0	10.20	1.61	0.202	0.798	0.81	4.87
M1	3926.9	518.5	159.5	7.57	3.25	0.158	0.842	0.54	6.48
M2	324.8	211.6	117.7	1.54	1.80	0.037	0.963	0.19	2.30
M3	567.4	126.9	46.5	4.54	2.73	0.102	0.899	0.12	1.49
G1	300.5	95.8	32.5	3.14	2.95	0.073	0.928	0.09	2.16
G2	398.0	245.9	53.5	1.62	4.60	0.039	0.961	0.22	5.38

For the calculations it is a simplification to treat the $3d^7$ configuration as three holes in a closed d shell. In the strong-field approach the d-wave functions are split by the cubic field into e and t_2 orbitals. The eigenfunctions in terms of $|l,m_l\rangle$ are

$$
\begin{aligned}
&|t_2,1'\rangle = |2,-1\rangle = -(|zx\rangle_d + i\,|yz\rangle_d)/\sqrt{2}\,,\\
&|t_2,0'\rangle = (|2,2\rangle - |2,-2\rangle)/\sqrt{2} = i\,|xy\rangle_d = |\zeta\rangle\,,\\
&|t_2,-1'\rangle = -|2,1\rangle = (|zx\rangle_d - i\,|yz\rangle_d)/\sqrt{2}\,,\\
&|e,\theta\rangle = |2,0\rangle = |3z^2-r^2\rangle_d/\sqrt{2}\,,\\
&|e,\varepsilon\rangle = (|2,2\rangle + |2,-2\rangle)/\sqrt{2} = |x^2-y^2\rangle_d\,,
\end{aligned}
\tag{3}
$$

where the prime indicates that the orbital momentum is an effective one. Following Thornley *et al.*,[22] the notation $|\zeta\rangle$ is introduced to avoid confusion in the formulas to be derived. The hole configuration for the ground state is the ${}^4T_1$ (t_2e^2) triplet. Higher energy states such as ${}^4T_2$ (t_2^2e) will be neglected. To write down the ground state of Fe_i^+ we introduce the following notation. An orbital state of ${}^4T_1$ will be written as a single Slater determinant $|abc|$. A spin state will be denoted as

$$
\begin{aligned}
&(|abc|[+++]) = |a^+b^+c^+|\quad (m_S=\tfrac{3}{2})\,,\\
&(|abc|[++-]) = (|a^+b^+c^-| + |a^+b^-c^+|\\
&\qquad + |a^-b^+c^+|)/\sqrt{3}\quad (m_S=\tfrac{1}{2})\,,
\end{aligned}
\tag{4}
$$

and similar expressions for the other two spin states. $[++-]$ means a symmetrized Slater determinant. Spin-orbit coupling mixes the spin $S=\frac{3}{2}$ and the effective orbital momentum $L'=1$ to $J=\frac{5}{2}$, $\frac{3}{2}$, and $\frac{1}{2}$. The ground state doublet, corresponding to $J=\frac{1}{2}$ is given in terms of $|m_{L'}\rangle\,|m_S\rangle$ by the vector coupling formula:

$$
\begin{aligned}
|m_J=+\tfrac{1}{2}\rangle = |+\rangle = {}&|1'\rangle\,|-\tfrac{1}{2}\rangle/\sqrt{6}\\
&-|0'\rangle\,|\tfrac{1}{2}\rangle/\sqrt{3} + |-1'\rangle\,|\tfrac{3}{2}\rangle/\sqrt{2}\,,\\
|m_J=-\tfrac{1}{2}\rangle = |-\rangle = {}&|-1'\rangle\,|\tfrac{1}{2}\rangle/\sqrt{6}\\
&-|0'\rangle\,|-\tfrac{1}{2}\rangle/\sqrt{3}\\
&+|1'\rangle\,|-\tfrac{3}{2}\rangle/\sqrt{2}\,.
\end{aligned}
\tag{5}
$$

In the notation as introduced in Eqs. (4) this is rewritten as

$$
\begin{aligned}
|m_J=+\tfrac{1}{2}\rangle = {}&(|1'\theta\varepsilon|[+--])/\sqrt{6}\\
&-(|0'\theta\varepsilon|[++-])/\sqrt{3}\\
&+(|-1'\theta\varepsilon|[+++])/\sqrt{2}\,,
\end{aligned}
\tag{6}
$$

and a similar formula for its Kramers conjugate state.

In terms of d orbitals the ground-state doublet of interstitial Fe^+ is finally written

$$
\begin{aligned}
|+\rangle = {}&(|-1\theta\varepsilon|[+--])/\sqrt{6}\\
&-(|\zeta\theta\varepsilon|[++-])/\sqrt{3}\\
&-(|1\theta\varepsilon|[+++])/\sqrt{2}\,,\\
|-\rangle = {}&-(|1\theta\varepsilon|[++-])/\sqrt{6}\\
&-(|\zeta\theta\varepsilon|[+--])/\sqrt{3}\\
&+(|-1\theta\varepsilon|[---])/\sqrt{2}\,.
\end{aligned}
\tag{7}
$$

The important difference with the theory for Ti^+, Fe^0, and Cr^+ is that in those cases there is no orbital degeneracy in the t_2 and e shells. The ground state is then given by a single Slater determinant.

In order to calculate the ligand hyperfine structure we

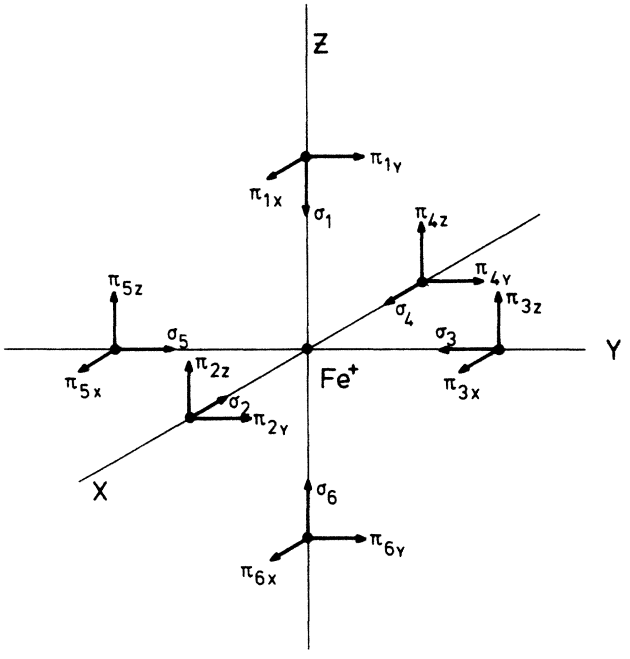

FIG. 3. Orientations of the σ and π ligand orbitals centered on the six atoms of a rhombic shell, symmetry $2mm$.

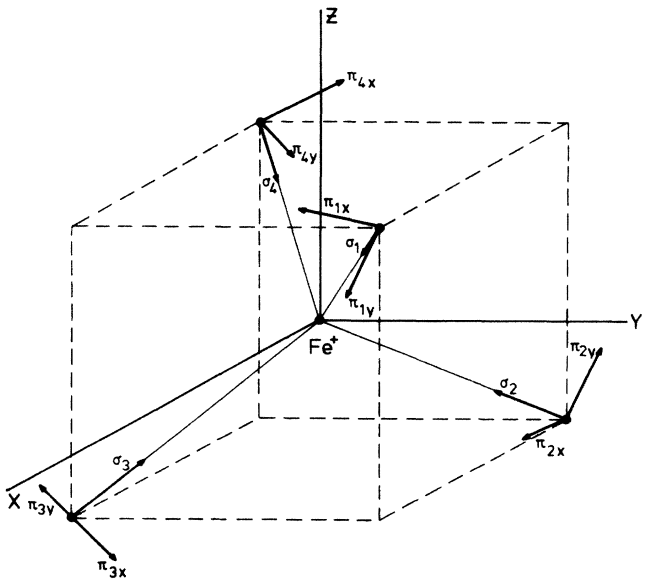

FIG. 4. Orientations of σ and π ligand orbitals centered on the four atoms of a trigonal shell. Directions of the orbitals centered on atom 1 are $\sigma_1=(-1,-1,-1)/\sqrt{3}$, $\pi_{1x}=(1,-2,1)/\sqrt{6}$, and $\pi_{1y}=(1,0,-1)/\sqrt{2}$.

must admix to the d orbitals of the central ion a linear combination of $3s$ and $3p$ orbitals of the surrounding lattice, belonging to the same irreducible representation. These molecular orbitals need to be constructed for every shell of ligand atoms. One can find the correct combination of ligand orbitals with the use of projection operators, a procedure which is outlined in Ref. 24 and applied in Refs. 13, 20, and 21. In order to project the ligand orbitals, one conveniently uses a (σ,π_x,π_y) coordinate system as illustrated in Figs. 3 and 4 for rhombic and trigonal class shells, respectively. In general, these are not identical to the coordinates used in Eq. (7). With respect to the (x,y,x) Cartesian coordinates, we find the following molecular orbitals for the $2mm$ (rhombic I) class:

$$
\begin{aligned}
&|xy\rangle=\alpha|xy\rangle_d+(1/\sqrt{2})\beta(s_1-s_6)+(1/\sqrt{2})\gamma(-z_1-z_6)+\tfrac{1}{2}\delta(z_2+z_3+z_4+z_5)+\tfrac{1}{2}\varepsilon(y_2+x_3-y_4-x_5)\ ,\\
&|yz\rangle=\alpha|yz\rangle_d+(1/\sqrt{2})\beta(s_2-s_4)+(1/\sqrt{2})\gamma(-x_2-x_4)+\tfrac{1}{2}\delta(x_1+x_3+x_5+x_6)+\tfrac{1}{2}\varepsilon(y_1+z_3-z_5-y_6)\ ,\\
&|zx\rangle=\alpha|zx\rangle_d+(1/\sqrt{2})\beta(s_3-s_5)+(1/\sqrt{2})\gamma(-y_3-y_5)+\tfrac{1}{2}\delta(y_1+y_2+y_4+y_6)+\tfrac{1}{2}\varepsilon(x_1+z_2-z_4-x_6)\ ,\\
&|3z^2-r^2\rangle=\alpha'|3z^2-r^2\rangle_d+(1/2\sqrt{3})\xi(2s_1+2s_6-s_2-s_3-s_4-s_5)+(1/2\sqrt{3})\kappa(-2z_1+2z_6+x_2+y_3-x_4-y_5)\ ,\\
&|x^2-y^2\rangle=\alpha'|x^2-y^2\rangle_d+\tfrac{1}{2}\xi(s_2-s_3+s_4-s_5)+\tfrac{1}{2}\kappa(-x_2+y_3+x_4-y_5)\ .
\end{aligned}
\tag{8}
$$

α^2 and α'^2 denote the amount of spin on the central Fe_i^+ ion in the t_2 and e orbitals. The other coefficients are the admixtures of spin on the ligands in a specific shell. The molecular wave function can only be normalized when the contributions of all ligand shells are added. In order to calculate the ligand hyperfine interaction we only have to consider one given ligand atom, say no. 1, because the other ligands in the shell are equivalent by symmetry. The contribution of ligand 1 can conveniently be rewritten in terms of s and p orbitals:

$$
\begin{aligned}
&|1\rangle=\alpha|1\rangle_d+(\varepsilon/2)|1\rangle_p-(i\delta/2)|-1\rangle_p\ ,\\
&|\zeta\rangle=\alpha|\zeta\rangle_d+(i\beta/\sqrt{2})|s\rangle-(i\gamma/\sqrt{2})|0\rangle_p\ ,\\
&|-1\rangle=\alpha|-1\rangle_d+(i\delta/2)|1\rangle_p+(\varepsilon/2)|-1\rangle_p\ ,\\
&|\theta\rangle=\alpha'|\theta\rangle_d+(\xi/\sqrt{3})|s\rangle-(\kappa/\sqrt{3})|0\rangle_p\ ,\\
&|\varepsilon\rangle=\alpha'|\varepsilon\rangle_d\ .
\end{aligned}
\tag{9}
$$

For the trigonal case, the contribution from atom 1 (Fig. 4) is in a similar treatment given by

$$
\begin{aligned}
|xy\rangle&=\alpha|xy\rangle_d+(\beta/2)|s\rangle-(\gamma/2\sqrt{3})|x+y+z\rangle_p\\
&\quad+(\delta/2\sqrt{6})|x+y-2z\rangle_p\ ,\\
|yz\rangle&=\alpha|yz\rangle_d+(\beta/2)|s\rangle-(\gamma/2\sqrt{3})|x+y+z\rangle_p\\
&\quad+(\delta/2\sqrt{6})|-2x+y+z\rangle_p\ ,\\
|zx\rangle&=\alpha|zx\rangle_d+(\beta/2)|s\rangle-(\gamma/2\sqrt{3})|x+y+z\rangle_p\\
&\quad+(\delta/2\sqrt{6})|x-2y+z\rangle_p\ ,\\
|\theta\rangle&=\alpha'|\theta\rangle_d+(\varepsilon/2\sqrt{6})|-x-y+2z\rangle_p\ ,\\
|\varepsilon\rangle&=\alpha'|\varepsilon\rangle_d+(\varepsilon/2\sqrt{2})|x-y\rangle_p\ .
\end{aligned}
\tag{10}
$$

On the M and G class shells we will comment later. For convenience the difference between α and α' will be neglected.

In the effective spin formalism the hyperfine interaction is written as: $\mathcal{H}=\mathbf{J}\cdot\overleftrightarrow{\mathbf{A}}\cdot\mathbf{I}$ with $J=\frac{1}{2}$ and eigenstates $|+\tfrac{1}{2}\rangle$ and $|-\tfrac{1}{2}\rangle$. Making the correspondence between this effective spin formalism and the ground state $|+\rangle, |-\rangle$ when defining $\mathcal{H}=\mathbf{N}\cdot\mathbf{I}$, one derives

$$
\begin{aligned}
A_{zz}&=2\langle+|N_z|+\rangle\ ,\\
A_{xx}&=2\,\mathrm{Re}\{\langle-|N_x|+\rangle\}\ ,\\
A_{yy}&=2\,\mathrm{Im}\{\langle-|N_y|+\rangle\}\ ,\\
A_{xy}&=2\,\mathrm{Re}\{\langle-|N_y|+\rangle\}\ ,\\
A_{zx}&=2\,\mathrm{Re}\{\langle-|N_z|+\rangle\}\ ,\\
A_{yz}&=2\,\mathrm{Im}\{\langle-|N_z|+\rangle\}\ .
\end{aligned}
\tag{11}
$$

The hyperfine structure operator $\mathbf{N}$ consists of three different contributions.

(a) Interactions with s electrons. The admixture of s electrons gives rise to the Fermi contact interaction and the Hamiltonian is written as

$$
\mathcal{H}=(\mu_0/4\pi)\tfrac{8}{3}\pi g_e g_N\mu_B\mu_N\left[\sum_i|\psi_i(0)|^2\mathbf{s}_i\cdot\mathbf{I}\right]\ ,
\tag{12}
$$

where the summation is over the single-particle orbitals and $s_i=\frac{1}{2}$. In the case of silicon the prefactor

$$
A_s=\tfrac{2}{3}\mu_0 g_e g_N\mu_B\mu_N|\psi_{3s}(0)|^2
$$

equals -4594 MHz (in frequency units).

(b) Interaction with p electrons. The interaction is given by

$$
\mathcal{H}=(\mu_0/4\pi)g_e g_N\mu_B\mu_N\langle r^{-3}\rangle_{3p}\sum_i(\mathbf{N}_i\cdot\mathbf{I})\ ,
\tag{13}
$$

with

$$
\mathbf{N}_i=\boldsymbol{l}_i-\kappa_c\mathbf{s}_i+\chi[l_i(l_i+1)\mathbf{s}_i-\tfrac{3}{2}(\boldsymbol{l}_i\cdot\mathbf{s}_i)\boldsymbol{l}_i-\tfrac{3}{2}\boldsymbol{l}_i(\boldsymbol{l}_i\cdot\mathbf{s}_i)]\ .
$$

Again the summation is over the occupied single-hole orbitals, $s_i=\frac{1}{2}$, $l_i=1$ (p electrons) and thus $\chi=\frac{2}{5}$. The first term represents the nuclear-spin–electron-orbit interaction. The second term accounts for the core polarization with κ_c an empirical constant. The remaining terms are the electron-spin–nuclear-spin dipolar interactions. In the case of silicon no reliable estimate for the core-

polarization constant κ_c can be given. Fortunately, the parameters to be determined, the admixture coefficients of ligand orbitals, are almost completely insensitive to changes in κ_c.[22] In the analysis κ_c was therefore taken to be 0. For silicon the prefactor

$$A_p=(\mu_0/4\pi)g_e g_N \mu_B \mu_N \langle r^{-3}\rangle_{3p}$$

equals -285 MHz.

(c) Dipolar interaction with distant electrons. Here we restrict ourselves to the dipole-dipole interaction between the d electrons on the central ion and the nuclear spins of the ligands. In the point dipole approximation it is determined by the parameter

$$A_d=(\mu_0/4\pi)g_e g_N \mu_B \mu_N (R^{-3})\alpha^2 , \tag{14}$$

with R the distance between central ion and ligand and α^2 the fraction of spin that is actually on the central ion. On principal axes the hyperfine tensor due to this dipolar interaction is given by

$$A_{zz}=2A_d, \quad A_{xx}=A_{yy}=-A_d .$$

For these operators the matrix elements given in Eq. (11) are to be calculated. We neglect contributions to the hyperfine tensor from atoms on other sites than the one considered, except the dipolar interaction with the central ion as given in (c). Since there are no matrix elements between a p and an s orbital, we can calculate the p and s contributions separately. The, very lengthy, calculations then give the following results: For rhombic symmetry,

$$\begin{aligned}
A_{zz}&=2A_d\alpha^2+A_s(\tfrac{1}{18}\beta^2+\tfrac{5}{27}\xi^2)\\
&\quad+A_p[-\tfrac{19}{90}\delta^2+\tfrac{11}{90}\varepsilon^2+\tfrac{2}{45}\gamma^2+\tfrac{4}{27}\kappa^2+(1/15\sqrt{2})\gamma\delta] ,\\
A_{xx}&=-A_d\alpha^2+A_s(-\tfrac{1}{9}\beta^2+\tfrac{5}{27}\xi^2)\\
&\quad+A_p[-\tfrac{1}{60}\delta^2-\tfrac{1}{60}\varepsilon^2-\tfrac{2}{45}\gamma^2-\tfrac{2}{27}\kappa^2+(11/30\sqrt{2})\delta\gamma] ,\\
A_{xy}&=A_p[\tfrac{4}{45}\varepsilon\delta-(3/10\sqrt{2})\varepsilon\gamma] ,\\
A_{yy}&=A_{xx}; \quad A_{yz}=A_{zx}=0 .
\end{aligned} \tag{15}$$

For trigonal symmetry,

$$\begin{aligned}
A_{zz}&=A_s\tfrac{5}{36}\beta^2+A_p[-\tfrac{7}{60}\delta^2-\tfrac{1}{90}\gamma^2-(19/45\sqrt{2})\gamma\delta] ,\\
A_{zx}&=A_d\alpha^2-A_s\tfrac{1}{36}\beta^2\\
&\quad+A_p[-\tfrac{7}{72}\delta^2-\tfrac{1}{10}\gamma^2-\tfrac{1}{18}\varepsilon^2+(3/20\sqrt{2})\gamma\delta] ,\\
A_{xx}&=A_{yy}=A_{zz}; \quad A_{xy}=A_{yz}=A_{zx} .
\end{aligned} \tag{16}$$

The most striking feature is that the Fermi contact interaction (terms with A_s) is no longer isotropic. Anisotropy did also arise in the case of Co^{2+} in an octahedral field, although in that case the anisotropy was only present if the excited state $^4T_1(t_2^2e)$ was taken into account.[22] On the other hand the interaction with p electrons does not give a traceless contribution to the hyperfine tensor A but contains an isotropic part as well. Therefore, it is not very useful to split the experimental tensor into a diagonal and an off-diagonal part. Finally, we note that there are more parameters describing the spin transfer to the ligand orbitals than measured data in the form of hyperfine tensor components. It is thus impossible to obtain the spin density in the orbitals separately. It is not even possible to determine the total amount of spin transferred from the central ion to a silicon lattice shell, chiefly because parameters with coefficients of either sign are summed.

Since for interstitial Fe^+ the important discussion is whether it is a localized or a delocalized defect, we attempted to find a minimum transferred spin density (MTSD). For that purpose a computer program was written around the routine E04WAF from the NAG program library, to find an extremum of the sum of squares of all admixture coefficients under the constraints given by Eqs. (15) and (16). The summation is over all coefficients for a shell, except α, because α^2 is the spin density on the central ion and depends on the total admixtures to all ligands and not just on the admixture to one specific ligand shell. α^2 was therefore set equal to some reasonable values, i.e., 0.5, 0.6, or 0.7. The allowed difference between α and α' is neglected. Because the distant dipolar interaction A_d depends on R, we have to assign each tensor to a specific shell. Since we have no *a priori* knowledge of the electronic structure, we can only make the assignment in an intuitive manner. We assign the tensor with the largest spin density in the one-electron linear combination of atomic orbitals (LCAO) analysis to the nearest shell with the appropriate symmetry. Thus T2 is assigned to the nearest-neighbor shell, R1 to the second, and so on. Therefore, the procedure outlined above computes that combination of parameters (the ligand admixture coefficients) that accounts for the observed hyperfine tensor, and that minimizes the total spin transfer to the corresponding ligand shell. A similar attempt to find a maximum spin transfer did not result in physically acceptable results. For $\alpha^2=\alpha'^2=0.6$ we obtained the results for the minimum transferred spin density to the whole shell of symmetry related neighbors as given in Table III. The results did not differ much for $\alpha^2=0.5$ or 0.7. It is noted that a fit to tensor T2 could only be found by taking the Cartesian tensor elements as negative. The overall sign of the tensors is quite important, taking the elements of R1 negative gives a minimum spin transfer of 18% in R1. Interchanging the shell assignment of T1 and T2 the total amount of spin transfer in T1 and T2 was also 5.7%. Comparing the figures as obtained by the LCAO and MTSD analysis, we note that the LCAO procedure tends to give slightly higher values

TABLE III. Calculated ligand admixture from the trigonal and rhombic hyperfine interactions. Given are values of spin transfer obtained from a simple one-electron LCAO treatment and the minimum transfer of spin density (MTSD) as obtained from the present calculations.

Tensor	LCAO (%)	MTSD (%)	Shell
T1	0.86	0.53	(2,2,2)
T2	4.3	5.2	(1,1,1)
R1	4.9	2.7	(2,0,0)

TABLE IV. Comparison of axial directions of *M*- and *G*-class tensors with pertinent directions of lattice sites. Given are angles between these directions. For the lattice sites the distances *d* to the central ion are given, as well as their shell numbers when ordering shells after their distance within each symmetry class.

Tensor	Axis	Position	No.	Angle	*d* (Å)
M1	(0.367,0.367,0.855)	(1,1,3)	1	6.0°	4.50
M2	(0.687,0.687,0.236)	(3,3,1)	2	0.4°	5.91
M3	(0.578,0.578,0.576)	(4,4,2)	4,5	15.7°	8.14
M3		(3,3,5)	6	14.5°	8.90
G1	(0.385,0.497,0.778)	(1,3,5)	2	12.9°	8.03
G2	(0.095,0.549,0.830)	(0.2,4)	1	8.8°	6.07
G2		(0.4,6)	3	5.5°	9.78

than the calculated minimum spin transfer.

So far we have limited our calculations to the rhombic and trigonal ENDOR tensors. In the case of the lower symmetry tensors M1–M3 and G1,G2, the analysis encounters further difficulties which we will now discuss. The correctly symmetrized molecular orbitals are projected in terms of s, σ, π_x, and π_y ligand orbitals. The iron ground state, on the other hand, is written with respect to x,y,z coordinates. Therefore one needs to express the molecular orbitals in x,y,z coordinates. In case of rhombic-I symmetry the two sets (x,y,z) and (π_x,π_y,σ) are almost identical (Fig. 3) and for trigonal symmetry the fixed relation is shown in Fig. 4. In the case of mirror plane (M) or general class (G) symmetry, the transformation between (π_x,π_y,σ) and (x,y,z) is not only dependent on the symmetry class but also on the specific shell of atoms considered. For example in a M class shell, atom 1 is positioned at (n,n,m) and the σ orbital points in the $[-n\ -n\ -m]$ direction. Therefore, for the shell containing $(1,1,-3)$ and the shell containing (3,3,1) a different set of orbitals is used. This implies that for these lower symmetry classes M and G no general expressions for the hyperfine tensor components can be given. A separate complete calculation has to be done for every possible shell of atoms, whereas the calculational effort does not diminish with lower symmetry. In the case of these lower symmetries even more parameters (ligand admixture coefficients) and independent hyperfine tensor elements are allowed that aggravate the calculations. Also it is questionable whether the numerical searching routine will still yield reliable results in these cases. Furthermore, the assignment of a hyperfine tensor to a shell of ligands can be subject to ambiguity.[13,20,21]

In the analysis of hyperfine interactions of Ti^+ and Cr^+ an interesting correlation between axial directions of hyperfine interactions and directions of neighboring silicon sites had been found for all M- and some G-class tensors.[20,21] From this correlation tentative assignments of tensors to shells of atom sites could be made. It was deduced that admixture of σ orbitals was far prominent, although π admixture was allowed by symmetry as well. In the present case a similar comparison can be made. In Table IV axial directions of M- and G-class tensors are compared with positions of pertinent lattice sites. Angles between the two directions are given. It follows that reasonable assignments can be made with nearby sites of the right symmetry. In the present case it is much less self-evident what effect σ orbitals will eventually produce in the hyperfine interaction. If we consider the given orbitals for rhombic and trigonal symmetry, Eqs. (8) and (10), we notice that admixture of σ orbitals in the doublet states is only allowed in the rhombic case. In Eq. (15) it directly gives rise to terms which are axial along the ligand direction. The effect for the triplet states is somewhat more complicated. Inspection of Eqs. (15) and (16) reveals that admixture of solely σ orbitals gives rise to both a small isotropic contribution and an anisotropic contribution which turns out to be also axial along the ligand direction, for trigonal as well as for rhombic symmetry. Although similar formulas for M- and G-class shells have not been derived for the reasons mentioned earlier, one may expect that they will exhibit a similar behavior. From the observed correlation in Table IV we may thus conclude that in the present case of the M- and G-class sites of Fe^+ there is a preference for σ admixture as well. Because of the much more complicated relation between ligand orbitals and hyperfine interaction than in the orbital singlet states of Ti^+ and Cr^+, even this simplification does not enable us to give a more exact estimate of the ligand admixture to these sites without tedious calculations.

In the case of Ti and Cr the analysis yielded a MTSD on the order of the result of the one-electron LCAO analysis. Also for the trigonal and rhombic shells in the present case results are only a little different. For these reasons we did not pursue the calculational efforts for the M- and G-class tensors and used the LCAO results as an approximation of the MTSD.

Summarizing, we conclude that from the present ENDOR experiments it follows that the transferred spin density from the interstitial Fe^+ ion to the ligand silicon atoms is at least 26%.

V. DISCUSSION

We have shown that the interstitial Fe^+ defect in silicon interacts strongly with the silicon lattice, as the electronic spin distribution can be measured over a volume of 98 atoms. From the hyperfine interactions we derived that a lower limit of the amount of transferred spin to these ligands is 26%. An upper margin of the spin transfer can only be estimated from the reduction of the observed isotropic hyperfine interaction of the ^{57}Fe ion with respect to the free ion. When using the calculated hyperfine interaction of the free ion by Watson and Free-

man,[25] one arrives at $|\psi(0)|^2=0.836$ (a.u.)$^{-3}$. From the experimental value $A=8.96$ MHz (Ref. 2) for Fe^+ in silicon, and using the formula $A=\frac{2}{3}\mu_0 g_e g_N \mu_B \mu_N |\psi(0)|^2$ one finds $|\psi(0)|^2=0.037$ (a.u.)$^{-3}$. This reduction by 95% is thought to give an estimate for the upper limit of the spin transfer. This conclusion is based on the assumption that the self-hyperfine interaction is entirely caused by exchange core polarization of the closed shells of s electrons, which in turn is proportional to the d localization on the central ion. It is not certain, though, how crude this approximation is.

When comparing the ^{29}Si ENDOR results of neutral iron in silicon[12,13] and the present results for Fe^+, some similarities attract attention. The hyperfine tensors of Si:Fe_i^+ labeled T1, T2, R1, and M1 have striking equivalents in the case of Si:Fe_i^0. In particular, in both cases a very anisotropic, almost traceless, trigonal tensor is observed, while the hyperfine tensor with largest trace corresponds in both cases to a ligand shell with rhombic symmetry. In this respect Si:Fe is clearly different from Si:Ti^+ (Ref. 20) and Si:Cr^+ (Ref. 21), where the tensor with largest trace has trigonal symmetry. On the other hand, for the lower symmetry (M- and G-type) ligand shells of Fe_i^+ we observe a pronounced preference for σ ligand admixture. A similar preference had just been found for Ti^+ and Cr^+, while Fe^0 exhibits no such effect at all. A further comparison of the ENDOR results of Fe^0, Ti^+, and Cr^+ is given in Refs. 21 and 26.

It is most interesting to compare our results with recent theoretical calculations by Katayama-Yoshida and Zunger[7,8] and by Beeler *et al.*[9]. From Refs. 7 and 8 we will only pay attention to the more reliable results of the self-interaction-corrected–local-spin-density (SIC-LSD) method. The results of the mere LSD method can be rejected because they do not produce the experimentally observed high-spin state ($S=\frac{3}{2}$) of Fe_i^+. The calculations[7,8] show that both Fe_i^0 and Fe_i^+ have comparable ionic charge, 0.37 and 0.57 electron, respectively. The effect of ionization of Fe_i^0 is that 0.8 hole is distributed throughout the crystal. As for the spin density, Refs. 7 and 8 calculated a delocalization of 38% for Fe_i^+ (29% for Fe_i^0) and Ref. 9 calculated 27% (12% for Fe_i^0). The delocalization percentages of Refs. 7 and 8 and Ref. 9 are not directly comparable, as Ref. 9 calculates the localized spin as the spin within a Wigner-Seitz atomic sphere, while the impurity orbital subspace used in the SIC-LSD calculations[7,8] may correspond to a different volume. Anyway, the results of both calculations are in accordance with our ENDOR measurements. Also both experiment and theory indicate that the spin density is more delocalized for Fe_i^+ than for Fe_i^0. It is noted that in the case of Fe_i^0 only e orbitals are involved, enabling the exact determination of the ligand admixture coefficients, rather than a minimum spin transfer. In the complicated case of Fe_i^+ it is not possible to determine exact ligand admixtures. Hopefully, future calculations will enable the direct determination of the ^{29}Si hyperfine tensor components so that a further comparison between theory and experiment will become possible.

ACKNOWLEDGMENT

This work received financial support from the Foundation for Fundamental Research on Matter (FOM).

[1]E. R. Weber, Appl. Phys. A **30**, 1 (1983).
[2]G. W. Ludwig and H. H. Woodbury, in *Solid State Physics,* edited by F. Seitz and D. Turnbull (Academic, New York, 1962), Vol. 13, p. 223.
[3]H. H. Woodbury and G. W. Ludwig, Phys. Rev. **117**, 102 (1960).
[4]F. S. Ham, Phys. Rev. **138**, A1727 (1965).
[5]F. S. Ham, in *Electron Paramagnetic Resonance,* edited by S. Geschwind (Plenum, New York, 1972), p. 1.
[6]H. Katayama-Yoshida and A. Zunger, Mater. Res. Soc. Symp. Proc. **46**, 111 (1985).
[7]H. Katayama-Yoshida and A. Zunger, Phys. Rev. B **31**, 7877 (1985).
[8]A. Zunger, in *Solid State Physics,* edited by H. Ehrenreich and D. Turnbull (Academic, Orlando, 1986), Vol. 39, p. 275.
[9]F. Beeler, O. K. Andersen, and M. Scheffler, Phys. Rev. Lett. **55**, 1498 (1985).
[10]J. J. van Kooten, G. A. Weller, and C. A. J. Ammerlaan, Phys. Rev. B **30**, 4564 (1984).
[11]C. A. J. Ammerlaan and J. J. van Kooten, Mater. Res. Soc. Symp. Proc. **46**, 525 (1985).
[12]S. Greulich-Weber, J. R. Niklas, E. R. Weber, and J. M. Spaeth, Phys. Rev. B **30**, 6292 (1984).
[13]D. A. van Wezep, T. Gregorkiewicz, E. G. Sieverts, and C. A. J. Ammerlaan, Phys. Rev. B **34**, 4511 (1986).
[14]K. Graff and H. Pieper, J. Electrochem. Soc. **128**, 669 (1981).
[15]J. J. van Kooten, Ph.D. thesis, University of Amsterdam, 1987.
[16]E. G. Sieverts, S. H. Muller, C. A. J. Ammerlaan, and E. R. Weber, Solid State Commun. **47**, 631 (1983).
[17]G. D. Watkins and J. W. Corbett, Phys. Rev. **134**, A1359 (1964).
[18]J. R. Morton and K. F. Preston, J. Magn. Reson. **30**, 577 (1978).
[19]J. Owen and J. H. M. Thornley, Rep. Prog. Phys. **29**, 675 (1966).
[20]D. A. van Wezep, R. van Kemp, E. G. Sieverts, and C. A. J. Ammerlaan, Phys. Rev. B **32**, 7129 (1985).
[21]R. van Kemp, E. G. Sieverts, and C. A. J. Ammerlaan, Phys. Rev. B **36**, 3528 (1987).
[22]J. H. M. Thornley, C. G. Windsor, and J. Owen, Proc. R. Soc. London, Ser. A **284**, 252 (1965).
[23]A. Abragam and B. Bleaney, *Electron Paramagnetic Resonance of Transition Ions* (Clarendon, Oxford, 1970).
[24]B. di Bartolo, *Optical Interactions in Solids* (Wiley, New York, 1968).
[25]R. E. Watson and A. J. Freeman, in *Hyperfine Interactions,* edited by A. J. Freeman and R. B. Frankel (Academic, New York, 1967), p. 53.
[26]E. G. Sieverts, D. A. van Wezep, R. van Kemp, and C. A. J. Ammerlaan, Mater. Sci. Forum **10-12**, 729 (1986).